Research Square

Preprints are preliminary reports that have not undergone peer review.
They should not be considered conclusive, used to inform clinical practice,
or referenced by the media as validated information.

Improving the spatial measurement of conflict exposure for population health research: Comparing kernel density estimation against conventional approaches in Mali

Mariame O. Ouédraogo

m.ouedraogo@mail.utoronto.ca

University of Toronto

Peter M. Macharia

Institute of Tropical Medicine Antwerp

Birama A. Ly

École de Maintien de la Paix Alioune Blondin BEYE

Hamidou Niangaly

Institut National de la Santé Publique

Rokia Sissoko

Independent Public Health and Development Consultant

Léa Dao

Cluster Santé, Organisation Mondiale de la Santé

Aboubakary Konaté

Office National de la Santé de la Reproduction

Erjia Ge

University of Toronto

Hilary K. Brown

University of Toronto

Diego G. Bassani

University of Toronto

Research Article

Keywords: Armed conflict, Health, Spatial analysis, Kernel density estimation, Mali, Sahel, Africa

Posted Date: November 9th, 2026

DOI: https://doi.org/10.21203/rs.3.rs-9588657/v2

License: This work is licensed under a Creative Commons Attribution 4.0 International License.
Read Full License

Additional Declarations: No competing interests reported.

Improving the spatial measurement of conflict exposure for population health research: Comparing kernel density estimation against conventional approaches in Mali

Mariame O. Ouédraogo[1], Peter M. Macharia[2, 3], Birama A. Ly[4, 5], Hamidou Niangaly[6], Rokia Sissoko[7], Léa Dao[8], Aboubakary Konaté[9], Erjia Ge[1], Hilary K. Brown[1,10*], Diego G. Bassani[1*]

1. Dalla Lana School of Public Health, University of Toronto, Toronto, Ontario, Canada
2. Department of Public Health, Institute of Tropical Medicine, Antwerp, Belgium
3. Population and Health Impact Surveillance Group, Kenya Medical Research Institute-Wellcome Trust Research Programme, Nairobi, Kenya
4. Faculté de Médecine et d'Odontostomatologie de l'Université des Sciences, des Techniques et des Technologies de Bamako, Bamako, Mali
5. Centre d'Analyse et de Recherche de l'Espace Sahélo-Saharien Modibo GOITA de l'École de Maintien de la Paix Alioune Blondin BEYE, Bamako, Mali
6. Département Études et Recherches, Institut National de la Santé Publique, Bamako, Mali
7. Independent Public Health and Development Consultant, Dakar, Senegal
8. Cluster Santé, Organisation Mondiale de la Santé, Bamako, Mali
9. Office National de la Santé de la Reproduction, Bamako, Mali
10. Department of Health and Society, University of Toronto Scarborough, Canada

*These authors contributed equally as supervisors to the lead author and as co-senior responsible authors.

Corresponding author: Mariame O. Ouédraogo

Email: m.ouedraogo@mail.utoronto.ca

Address: Dalla Lana School of Public Health, University of Toronto, 55 College St, Toronto, Ontario, M5T 3M7, Canada

Abstract word count: 334 / 350

Full text word count (excluding figures and tables): 4996 / 5000

ABSTRACT

Background: Nuanced measures of armed conflict exposure are essential for understanding its health impacts. Common approaches to operationalizing conflict, such as calculating event or fatality rates within administrative boundaries or using a fixed radius around events to capture their spatial influence, can obscure important spatial and temporal patterns of conflict. Using Mali as a case study, we constructed a conflict intensity measure based on kernel density estimation (KDE) and compared it with standard approaches by examining population exposure and associations with key reproductive, maternal, and child health (RMCH) outcomes.

Methods: We compiled georeferenced conflict events from global datasets and used kernel density estimation (KDE) to create annual 10 × 10 km conflict-intensity surfaces for 2000–2024, aggregated to district and health-facility levels. We also measured conflict exposure as district-level event and fatality rates, and the number of events and fatalities within 50 km of a facility. For selected years (2013, 2018, and 2023), we compared the proportion of population subgroups classified as exposed to conflict across approaches, using percent agreement and Cohen's Kappa. We also examined associations between conflict measures and key RMCH indicators, using Spearman correlations and model-fit metrics (coefficient of determination (pseudo-R^2) and Akaike Information Criterion (AIC)).

Results: Across years, we found variability in the estimated proportion of the population exposed to conflict, depending on the conflict definition used. Agreement in classifying conflict-affected population groups was on average moderate, with kappa values ranging from 0.37 in 2023 to 0.77 in 2018. KDE revealed a log-linear dose-response relationship between conflict

intensity and selected RMCH indicators in 2013 and 2018, with correlation coefficients ranging from 0.31 to 0.74. Standard approaches showed weaker relationships, with correlations between -0.284 and 0.69. For most RMCH indicators, KDE produced higher pseudo-R^2 values and lower AIC values than the standard approaches in facility-level analyses.

Conclusions: KDE showed stronger ecological associations with RMCH outcomes and better model fit at the facility level than the standard methods. Its performance across conflict settings and at finer spatial scales remains to be explored.

KEYWORDS

Armed conflict; Health; Spatial analysis; Kernel density estimation; Mali; Sahel; Africa

BACKGROUND

In 2024, the world saw 61 active state-based armed conflicts, the highest number since 1989 [1]. By the end of 2025, one in six people lived in conflict-affected areas [2] and 117 million had been forcibly displaced by armed conflicts [3]. These events have far-reaching negative impacts on individuals, communities, and societies, with significant consequences for health [4]. Beyond the direct health impacts of conflicts, such as injuries, trauma, and death [5], increasing evidence indicates that most health consequences attributable to conflicts result from indirect pathways [6], via the destruction of key infrastructure and equipment, disruption of medical supply chains, and loss of vital human resources for the provision of health services [6, 7]. Additionally, conflicts exacerbate health inequities by widening socioeconomic disparities and increasing communities' exposure to overcrowding, poor nutrition, and inadequate water and sanitation [5, 6]. The consequences of armed conflicts on health are particularly profound for vulnerable groups, including women of reproductive age and young children, with studies showing reductions in maternal and child health service utilization, increases in adverse birth outcomes such as low birth weight, and higher mortality rates among these populations [8, 9].

Nuanced measures of conflict exposure are necessary to conduct research to support efficient planning and resource allocation for health programs and policies, as well as for humanitarian response. Measuring a multi-dimensional and subjective construct, such as conflict exposure, is challenging and best approached through primary data collection. Logistical and security constraints, however, often make conducting surveys and interviews infeasible. Consequently, there has been growing interest in using available secondary data on armed conflict to measure exposure and severity.

Many studies have defined conflict exposure using a threshold number or population-standardized rate of events (attacks, fatalities, or displaced people) within a specified area (a district or region)[10, 11]. Others have extended this approach by measuring conflict severity as the number or rate of conflict-related events, treated as a categorical or discrete variable [11–14]. Finally, studies with a focus on individual- or small-area impacts have used a fixed radius (50 kilometers) around households or communities to determine the extent of their proximity to conflict [15–19]. Beyond enabling measurement of conflict presence and severity, this approach recognizes that conflict events may indirectly affect health-seeking behaviors and outcomes beyond their immediate locations.

Although these approaches have been widely used, they suffer from drawbacks. The threshold of conflict-related event counts, or rates, used to determine exposure is subjective. Furthermore, relying on exposure measures based on administrative units may introduce the modifiable areal unit problem, meaning that summary measures are influenced by the spatial scale [20]. Conversely, the fixed-radius extent is determined by the researcher and assumes that all events, regardless of severity, have the same spatial influence (an event resulting in 100 casualties will affect an area in the same way as one causing no deaths). Further, the approach applies the same radius regardless of whether events occur in a remote, sparsely populated area or a densely populated area. Taking population size into account is important, as a conflict event may exert a distinct influence depending on an area's population density.

In response to these limitations, the use of kernel density estimation (KDE) to model both direct and indirect exposure to armed conflict continuously across space has been explored [21]. KDE is a smoothing method that transforms a point pattern of events into a continuous surface representing the density of those events [22]. This method has been extensively applied across various fields, ranging from epidemiology, to assess the spatial relative risk of health outcomes [23–25] to criminology, to support crime hotspot mapping and prediction [26, 27].

In a recent study by Tapsoba, KDE was used to examine the effects of armed conflicts on infant mortality in Côte d'Ivoire and Uganda by comparing a KDE-generated conflict exposure with exposure based on residence within a fixed 50-km radius of a conflict event [21]. Using the KDE approach, infant mortality was six percentage points higher among Ivorian children and two points higher among Ugandan children exposed to conflict, compared to unexposed children. However, in both contexts, there was no statistically significant difference in infant mortality between children living within 50 km of a conflict event and those living farther away. This work highlighted that a more nuanced appraisal of the health impacts of conflicts could potentially be achieved using KDE.

As evidence supporting the use of KDE to define conflict exposure remains limited, this paper aimed to examine whether KDE can improve the measurement of armed conflict dynamics for use in population health research. We first generated annual conflict intensity surfaces using KDE for Mali, a country that has been experiencing a complex, multifaceted, and highly dynamic conflict since 2012. We then compared KDE with the most common approaches to measuring conflict exposure and severity (the rate of conflict-related events or fatalities within

administrative boundaries and a fixed radius around health facilities to count events or fatalities). Comparison consisted of examining how conflict exposure measures derived from these methods classified population groups exposed to conflict, as well as how they related to key reproductive, maternal, and child health (RMCH) outcomes.

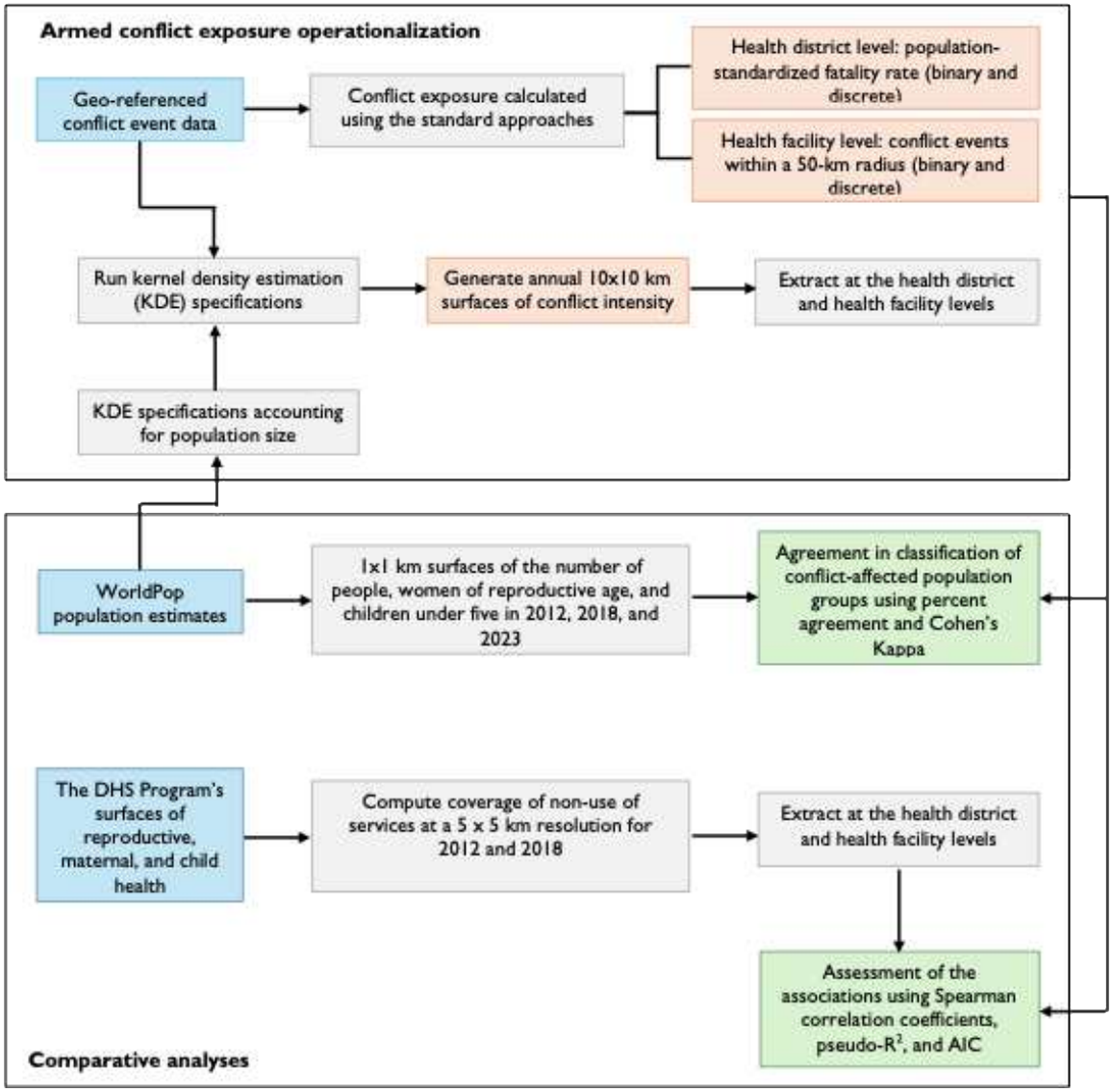
METHODS

Study area

This study was conducted in Mali, a landlocked country in West Africa situated on the Sahelian strip (Supplementary materials, section 1). The armed conflict, which started in 2012, is marked by terrorism, inter-ethnic violence, and political instability, and has had significant impacts on the well-being of civilians, limiting their access to basic social and health services [28–32].

Overview of methods

The operationalization of armed conflict exposure using KDE and standard approaches is summarized in Figure 1.



159

160 **Figure 1.** Flow chart of the steps adopted to produce the conflict measures using kernel density
161 estimation and the standard approaches, and testing their agreement and association with
162 reproductive, maternal, and child health indicators.

163

Data sources and processing

1. Conflict events

This study relied on publicly available georeferenced data on armed conflict events. The Armed Conflict Location and Event Data (ACLED) [33, 34] and the Uppsala Conflict Data Program (UCDP) [35, 36] are global references for conflict data. The UCDP adopts a strict definition of armed conflict, which must meet the threshold of 25 deaths annually to be included in the dataset. Recorded events are those that resulted in at least one fatality. In contrast, ACLED has a broader scope, capturing both events that led to and did not lead to fatalities, which is particularly relevant as some armed perpetrators purposefully terrorize populations without killing them [37]. For this study, we combined both datasets to include conflict events regardless of whether casualties occurred. Several steps were taken to merge the two datasets and ensure alignment of conflict event types captured (supplementary material, section 2). We restricted our datasets to events that occurred between 2000 and 2024 to capture the pre-conflict years as well as the different phases of conflict progression. The merged datasets included events with precise coordinates and the date of occurrence (day, month, and year). All duplicates (events sharing the same location, date, number of casualties, and similar event description) were merged. In cases where the duplicates had differing fatality counts, we used UCDP estimates, given UCDP's thorough quality appraisal system, which makes it superior to ACLED in reporting fatality counts [38].

2. Population size

We used annual gridded population estimates at a 1x1 km resolution produced by WorldPop between 2000 and 2024, inclusively [39]. Their estimates are produced using machine learning

methods applied to various geospatial covariates and satellite imagery to disaggregate population counts from census and other population-level microdata from areal units to 1x1 km grid cells. Details on the methods employed by the authors to produce the surfaces can be found elsewhere [39]. Population count surfaces were used at two distinct stages of analysis (Figure 1). Annual population count surfaces were first used to calibrate the KDE models for each year from 2000 to 2024. Population count surfaces for selected years were subsequently used to estimate the total population, as well as the number of women of reproductive age (15-49 years) and children under 5 years old exposed to conflict. We selected three time points (2013, 2018, 2023). These points were chosen to represent populations exposed to different phases of the armed conflict progression, but also to align as much as possible with the available health indicators presented below.

3. Reproductive, maternal, and child health indicators

We used spatially interpolated surfaces of the coverage of key RMCH indicators generated by the Demographic and Health Surveys (DHS) Program [40, 41]. The surfaces, which are publicly available [42], were produced using a Bayesian geostatistical approach that combined DHS survey data with spatial datasets capturing population density, urbanization levels, and climate-related characteristics; their construction is detailed elsewhere [40, 41]. The modeled surfaces for Mali were generated for years 2013 and 2018, using DHS 2012/13 and DHS 2018 data, respectively, at a resolution of 5 x 5 km, and captured the proportion of use of the following policy-relevant RMCH indicators: demand for family planning satisfied by modern methods, effective antenatal care (ANC) visits (defined as a minimum of four ANC contacts during pregnancy), institutional delivery, and third dose of diphtheria-tetanus-pertussis vaccine (DTP3)

among children 12 – 23 months. We derived surfaces for lack of access to these services by subtracting the modeled coverage values from 1 [43], producing the following indicators: unmet need for family planning among women of reproductive age, suboptimal ANC, non-institutional delivery, and missed DTP3 vaccination. We then aggregated the surfaces to the community health center catchment area and the health district levels by calculating the population-weighted mean. Community health centers serve as the primary point of contact with the healthcare system. Each center's catchment area extends up to a 15-kilometer radius to serve a population of 5,000 to 10,000. Each community health center is linked to a referral health center. A health district regroups a referral health center with its network of community health centers to ensure delivery of primary care [44]. For simplicity, throughout the rest of the article, community health centers are referred to as health centers. Our analysis included the 1,632 health centres and 68 health districts recorded in 2023; the coordinates of facilities and shapefiles of health districts were obtained directly from the Ministry of Health.

Kernel density estimation

Kernel density estimation (KDE) is a non-parametric method that allows estimation of an underlying probability density function (PDF) f of a point pattern dataset [22, 45]. The density estimation consists of constructing an estimate of f based on a representative sample of random realizations $\{x_1, \dots, x_n\}$ of a process X. In its simplest form, KDE is expressed as:

$$\hat{f}(x) = \sum_{i=1}^{n} \frac{1}{nh} K\left(\frac{x - x_i}{h}\right), \quad (1)$$

where a PDF $\hat{f}(x)$ is obtained by counting the contributions of random realizations under a fixed bandwidth h and a kernel function K. The bandwidth corresponds to the smoothing parameter and controls the spread or circle of influence. The kernel function controls the contribution of

each realization to the density function. One of the most common kernel functions used is the Gaussian function $K \sim (0,\ h)$[21]. The density estimate is obtained by summing all contributions across all *n* events, as per equation (1). The density function can be multiplied by the number of events *n* to obtain the intensity function, which gives the expected number of events per unit area [46].

The PDF can be extended to space-time KDE by using a three-dimensional matrix with longitude, latitude, and time:

$$\hat{f}(\bar{x}) = \sum_{i=1}^{n} \frac{1}{nH} K\left(\frac{\bar{x} - \bar{x}_i}{H}\right), \quad (2)$$

where $\bar{x}$ and $\bar{x}_i$ are d-dimensional vectors, H is a d x d symmetric matrix of smoothing parameters: $H = \begin{pmatrix} h_s & 0 & 0 \\ 0 & h_s & 0 \\ 0 & 0 & h_t \end{pmatrix}$, where we can assume that the latitude and longitude dimensions have the same smoothing parameter h_s and that the time dimension has a smoothing value of h_t [21].

1. Spatio-temporal bandwidth selection

We used an adaptive bandwidth that adjusted the radius or circle of influence according to the number of events (supplementary material). An adaptive bandwidth is well suited to representing densities for processes with substantial spatial and temporal variations [45]. A bootstrap method in conjunction with the mean integrated squared error (MISE) was used to determine an appropriate adaptive spatio-temporal bandwidth [47].

In selecting the period over which to calculate the spatio-temporal bandwidth, it was important to ensure adequate representation of the underlying process, balance under- and over-smoothing, and minimize the MISE and the computation time [47]. Several time periods within our study window (2000 to 2024) were tested, and we determined that using conflict events that occurred from 2013 to 2018 provided a balanced pilot spatio-temporal bandwidth. This decision was based on comparisons, made by authors familiar with the Malian conflict, of maps generated across different time periods in distinguishing meaningful hotspots from random noise.

2. Spatio-temporal windows

Assuming that an event's contribution to the PDF will not extend infinitely over space or time [21], we used spatial and temporal windows to truncate the kernel beyond the bandwidth distance. This was done by restricting to events that occurred within a defined spatial and temporal interval to compute conflict intensity at a specific space-time point (supplementary material, section 3).

3. Accounting for fatalities and population size

The KDE formula presented in (2) was adapted to account for the number of fatalities as well as population size as weights (supplementary material, section 3). The number of fatalities served as the key input to capture event intensity [21], while annual population counts from WorldPop produced from 2000 to 2024 were used to control the influence of each conflict event. Considering conflict dynamics in the Malian context [48] and nationwide surveys on public perceptions of the conflict [49], we assumed that events in densely populated areas would exert less influence than those in rural areas.

4. Edge correction

To account for edge effects near country boundaries [46, 50], we applied Diggle's edge-correction method. This approach weights each event by the inverse of the proportion of its kernel that falls within the study boundaries. We implemented the edge correction using Monte Carlo sampling [51]. For each conflict event location, 1,000 random points were generated to represent the kernel's spatial spread under an adaptive bandwidth, and the proportion of points falling within the country's boundaries was used to compute the corresponding weight for each event.

5. KDE specifications

We specified several KDE models to assess how key parameters, including spatial and temporal bandwidths and windows, as well as population-size adjustment, affected conflict intensity estimates. The models were implemented using the *pdfCluster* package in R version 4.5.2 [52]. Table 1 summarizes the models tested. For each model specification, we generated annual conflict intensity surfaces at a 10×10 km resolution. All models used an adaptive spatial bandwidth and incorporated fatality weights and edge correction. In sensitivity analyses, we varied spatial and temporal window lengths and reference points and accounted for temporal bandwidths (supplementary material, section 3). To compare the different model specifications, we examined the distribution of conflict-intensity values across years and assessed predictive criteria, namely the Mean Absolute Error (MAE) and Root Mean Squared Error (RMSE).

A series of maps illustrating conflict intensity from 2000 to 2024 was created. All surfaces were projected to UTM Zone 29 (EPSG:32629) and rescaled to kilometers. To align with the years for which RMCH indicators were available, we also summed the conflict intensity values for 2013 and 2018 within the health center's catchment areas and health districts.

Table 1. List of tested Kernel Density Estimation (KDE) models

	KDE parameters			
	Spatio-temporal window	**Spatio-temporal bandwidth**	**Population adjustment**	**Edge correction**
Model 1	No spatial window Temporal window of 364 days	Adaptive spatial bandwidth No temporal bandwidth	Yes	Yes
Model 2	No spatial window Temporal window of 364 days	Adaptive spatial bandwidth No temporal bandwidth	No	Yes
Model 3	No spatial window Temporal window of 364 days	Adaptive spatio-temporal bandwidth	Yes	Yes
Model 4	No spatial window Temporal window of ± 182 days	Adaptive spatio-temporal bandwidth	Yes	Yes
Model 5	Spatial window of 500 km Temporal window of 364 days	Adaptive spatial bandwidth No temporal bandwidth	Yes	Yes

<u>Comparison of KDE with standard approaches</u>

We considered three of the commonly used ways to operationalize armed conflict: conflict-related event rates, conflict-related fatality rates, and the fixed-radius approach. For each health district, we computed conflict-related event and fatality rates, expressed as the cumulative

number of events and fatalities, respectively, per 100,000 population. We also classified health districts as exposed to conflict if at least one event or one fatality per 100,000 population occurred [11] (Table S1). We also measured conflict severity by treating event and fatality rates as discrete variables.

At the health center level, we used the fixed-radius approach. In line with past work, we used a 50-km radius around each conflict event to determine exposure [15, 17, 18]; health centers were classified as exposed if they were located within a 50-km radius. We additionally calculated the total number of conflict events occurring within a 50-km radius of each health facility.

We first compared the KDE-based conflict exposure metric with selected standard approaches by examining the agreement in the exposure to conflict classification of the general population, women of reproductive age, and children under five. Any population count cell within a health district with at least one event per 100,000 population was classified as exposed. Cells were also grouped into unexposed and exposed according to the one fatality per 100,000 population threshold for health districts. Similarly, populations that fell partly or entirely within 50 km of a conflict event were categorized as exposed. Under the KDE approach, we defined conflict-intensity cells as moderately to severely exposed if they fell within the fourth or fifth quintile of KDE values (Figure S10). We then intersected these polygons with the population count surfaces to identify populations moderately or severely exposed to armed conflict. This spatial extraction was conducted using the *exactextractr* package [53], which calculates the fraction of each grid cell that overlaps with a specified polygon. The level of agreement between the KDE-based and the standard approaches was assessed using percent agreement and Cohen's Kappa [54]. Cohen's

Kappa values were interpreted according to the following scale: ≤ 0 indicates no agreement; 0.01–0.20 represents none to slight agreement; 0.21–0.40 is considered fair; 0.41–0.60 as moderate; 0.61–0.80 as substantial; and 0.81–1.00 as almost perfect agreement [54].

We subsequently assessed how conflict exposure metrics derived from standard approaches and KDE relate to key RMCH indicators for the years 2013 and 2018 at the level of the health districts and health centers. RMCH indicators were not available for 2023. We generated scatter plots for the logit-transformed RMCH coverage against the conflict exposure metrics. To identify the direction and strength of the associations between armed conflict measures and RMCH coverage, we computed Spearman rank correlation coefficients. We also fitted mixed-effects models with region as a random effect to derive key model fit metrics: pseudo coefficient of determination (pseudo-R^2) and Akaike Information Criterion (AIC)[55] .

RESULTS

Spatial and temporal distribution of armed conflict events in Mali

Our analyses included 6,908 unique conflict-related events reported between 2000 and 2024. The ACLED dataset contributed approximately 67% of the events. In the early 2000s, the security situation in Mali was characterized by sporadic conflict-related events (Figure S2). The year 2012 marked an escalation in violence, predominantly in the northern regions. A reduction in conflict intensity was observed in 2014 and 2015, with a decrease in reported fatalities. Since 2020, the conflict has become more widespread and intensified, affecting all regions of the country. Most (46%) events were battle-related, followed by violence against civilians (40%). Explosions and remote violence started to increase exponentially in 2018 (Figure S3).

Kernel density estimation

The spatial and temporal bandwidths were estimated at 63.2 km and 343.9 days, respectively. We found no significant differences among the five KDE models tested under different assumptions. Across all five models, the maps similarly highlighted areas with the highest conflict intensity (Figures S5 – S8). Box-plots of the overall distributions of conflict intensity values (Figure S9) along with prediction criterion values (Table S3) further indicated substantial overlap across the models. Given these results, we decided to use the KDE surfaces generated under Model 1 (Figure 2) to conduct the comparative analyses with the standard approaches.

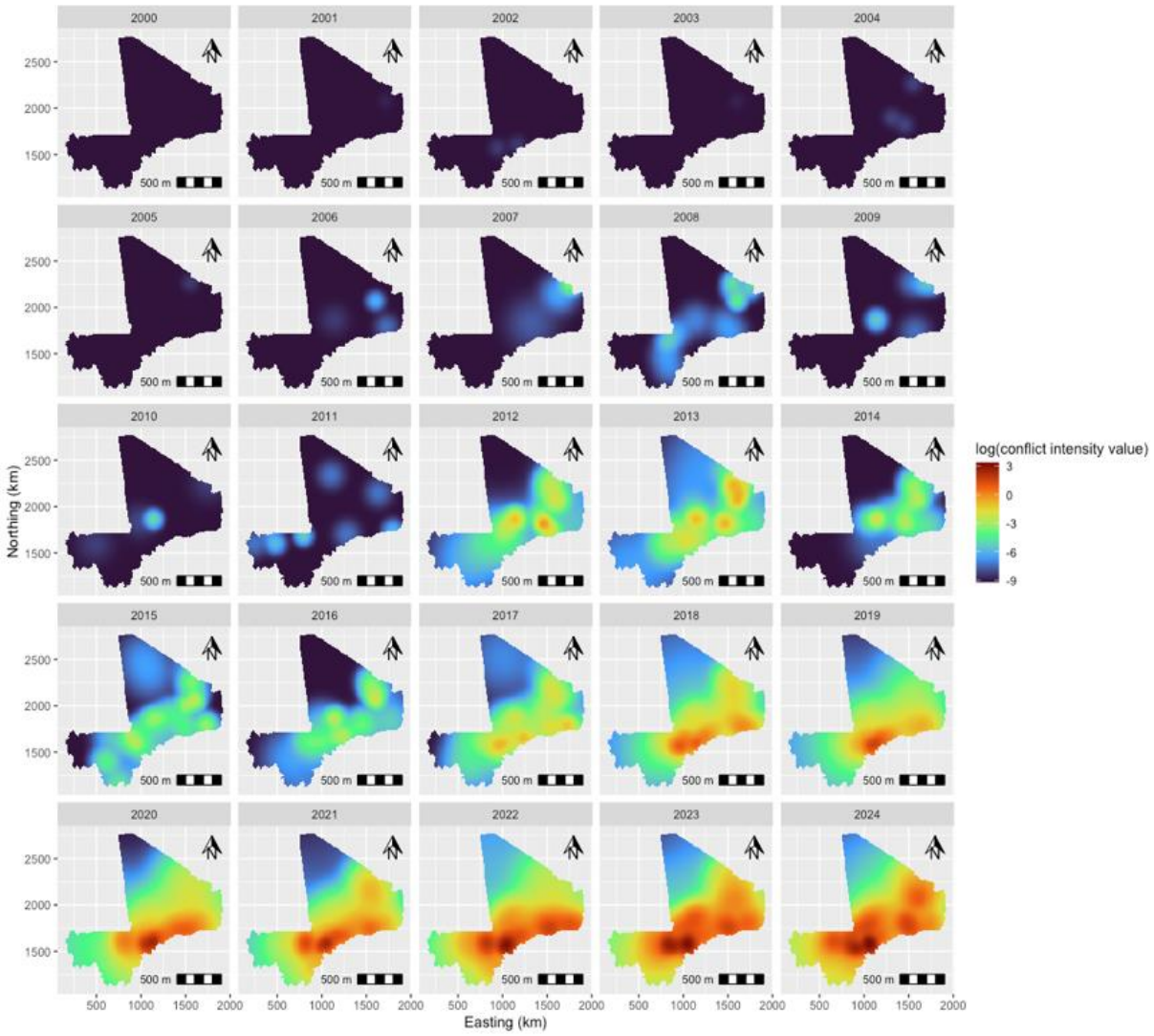


Figure 2. Annual conflict intensity surfaces obtained with population- and fatality-adjusted kernel density estimation, Mali 2000 to 2024

Kernel density estimation versus standard approaches

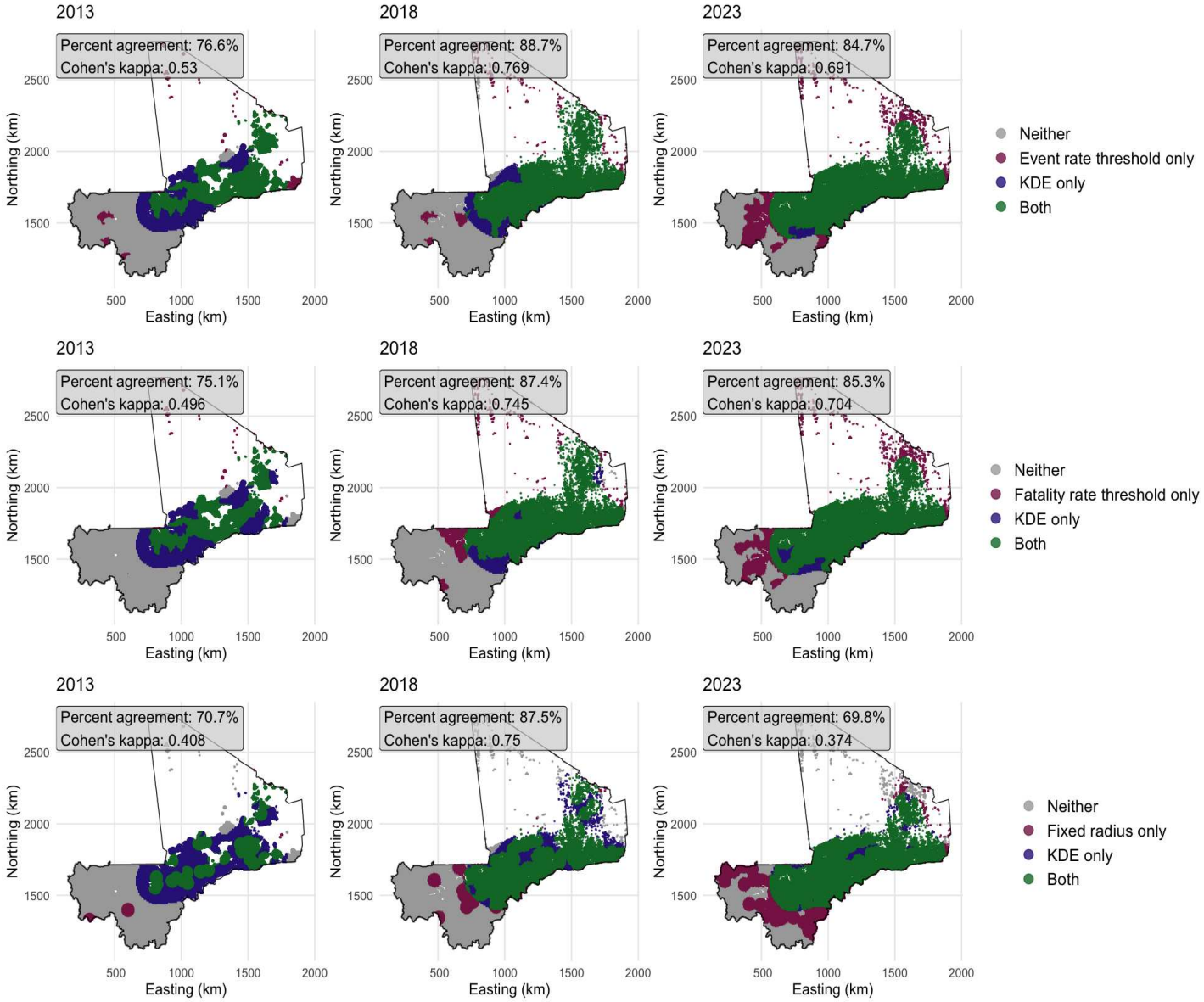
1. Population groups exposed to armed conflicts

Table 3 summarizes the distribution of populations classified as exposed to armed conflict at a pixel level by exposure definition. In 2013, the KDE approach and standard fixed-radius approach estimated the population exposed to conflict to be around 35%. In contrast, using either

a conflict-related event threshold or a fatality-rate threshold yielded an estimate of approximately 15%. In 2018, KDE identified 31% of the population groups exposed either moderately or severely to conflict compared to 23% to 36% for the standard approaches. Estimates of the population groups exposed to conflict were similar across the KDE approaches and two of the standard approaches, ranging from 37% to 40%. Under the fixed-radius approach, however, up to 87% of the population was classified as exposed to armed conflict in that year.

The pixel-agreement plot (Figure 3) shows that the percent agreement between the KDE approach and the standard ones ranged between 70% and 89%. Corresponding Cohen's kappa values ranged from 0.37 to 0.77, indicating fair to substantial agreement across the years. Agreement patterns for women of reproductive age and children under five were similar (Figures S12 and S13).

388



389 **Figure 3.** Comparison of kernel density estimation (KDE) and the standard approaches in the

390 general population estimated to be exposed to armed conflict. **Legend:** The standard approaches

391 considered from top to bottom are the conflict event rates, the fatality rates, and the fixed radius.

392 The agreements for the years 2013, 2018, and 2023 are displayed. The years' respective percent

393 agreement and Cohen's kappa values are also provided.

394

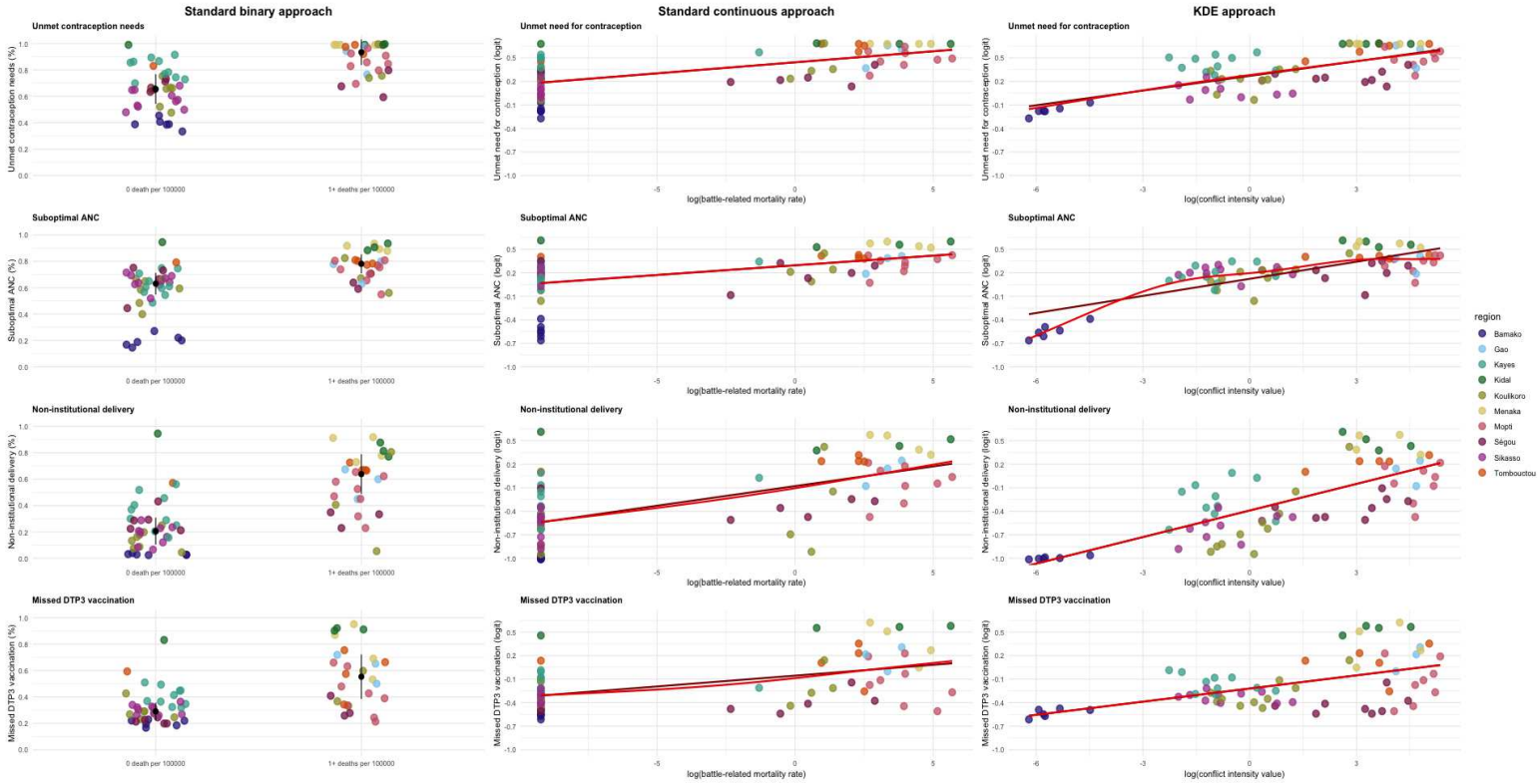
Table 3. Distribution of conflict-affected population subgroups (count in units of 10,000 and percentage) identified using the standard approach and the KDE approach

	Total population N x 10,000 (%)			Women of reproductive age N x 10,000 (%)			Under-five children N x 10,000 (%)		
	2013	**2018**	**2023**	**2013**	**2018**	**2023**	**2013**	**2018**	**2023**
Total	1,639.5 (100.0)	2,007.3 (100.0)	2,335.3 (100.0)	391.0 (100.0)	435.53 (100.0)	521.37 (100.0)	325.57 (100.0)	373.27 (100.0)	408.51 (100.0)
KDE approach									
Moderate or severe exposure (Q4 or Q5)	569.7 (34.7)	618.79 (30.8)	856.93 (36.7)	131.99 (33.7)	134.90 (30.9)	192.24 (36.8)	113.75 (34.9)	156.62 (30.9)	150.63 (36.8)
Standard approaches									
Health districts with at least one conflict event per 100,000 population	249.2 (15.2)	461.6 (22.9)	941.4 (40.3)	58.4 (15.0)	100.6 (22.9)	211.2 (40.3)	49.7 (15.2)	86.2 (22.9)	165.5 (40.3)
Health districts with at least one conflict-related fatalities per 100,000 population	231.4 (14.1)	507.7 (25.3)	904.8 (38.7)	54.6 (14.0)	110.7 (25.3)	202.9 (38.7)	45.3 (13.9)	94.9 (25.3)	159.0 (38.7)
At least one conflict event within a 50-km radius	568.71 (34.6)	716.25 (35.7)	2,027.92 (86.9)	141.99 (36.3)	155.82 (35.9)	452.79 (87.2)	105.3 (32.3)	133.55 (35.9)	354.79 (87.2)

2. Association between armed conflict and reproductive, maternal, and child health indicators

a) Health district level

The correlation coefficients for the association between KDE-specified conflict intensity and RMCH indicators were consistently higher than those for the standard approaches considered (Table 4). Across all four RMCH indicators, conflict measures, and time points, health districts with greater conflict exposure had, on average, higher proportions of women and children under five who underused key health services than districts with lower exposure (Figures 5, S16 - 18). Although in most cases the R^2 values were slightly higher for models using KDE-based conflict exposure than for those using standard approaches in 2013, the positive AIC difference indicated that the standard approaches provided a better model fit. In contrast, in 2018, higher R^2 values and a negative AIC difference indicated that models using KDE-based conflict exposure provided a better fit than the standard approaches. These models showed near-log-linear relationships in which increases in log-scaled conflict intensity were associated, on average, with lower levels of ANC, facility delivery, and DTP3.



413

414 **Figure 5. Association between conflict exposure measures and reproductive, maternal, and child health outcomes at the health**
415 **district level in 2018. Legend:** The left column displays RMCH indicator (%) distributions by the binary conflict exposure, defined as
416 the occurrence of at least one fatality per 100,000 population. The middle column shows distributions of the RMCH indicator (logit)
417 by fatality rates on the log scale. The right column presents distributions of the RMCH indicator (logit) by continuous conflict
418 intensity on the log scale, estimated using kernel density estimation (KDE). The linear regression lines are shown in light red, and the
419 non-linear lines from generalized additive models are shown in dark red.

Table 4. Spearman correlation coefficients and model fit metrics for the association between conflict exposure measures and reproductive, maternal, and child health outcomes at district and facility levels in 2018

		Health district level				Health facility level		
		ρ	**Pseudo-R^2**	**ΔAIC**		**ρ**	**Pseudo-R^2**	**ΔAIC**
Unmet contraception need	At least one event per 100,000	0.570	0.002	-24912.9	At least one event within 50-km buffer	0.421	0.003	-39268.9
	Log(number of events per 100,000)	0.675	0.114	18657.3	Log(number of events within 50-km buffer)	0.424	0.004	-39284.8
	At least one fatality per 100,000	0.655	0.056	6695.76	At least one fatality within 50-km buffer	0.427	0.006	-16938.3
	Log(number of fatalities per 100,000)	0.652	0.092	13476.6	Log(number of fatalities within 50-km buffer)	0.424	0.008	-16877.1
	Log(conflict intensity value)	0.626	0.146	0.0	Log(conflict intensity value)	0.553	0.136	0.0
Suboptimal antenatal care	At least one event per 100,000	0.574	0.036	-2082.4	At least one event within 50-km buffer	0.450	0.003	-14948.8
	Log(number of events per 100,000)	0.646	0.134	1125.6	Log(number of events within 50-km buffer)	0.454	0.004	-14778.6
	At least one fatality per 100,000	0.562	0.050	-2105.65	At least one fatality within 50-km buffer	0.388	0.000	-9059.8
	Log(number of fatalities per 100,000)	0.599	0.077	-543.08	Log(number of fatalities within 50-km buffer)	0.395	0.001	-9014.3
	Log(conflict intensity value)	0.672	0.331	0.0	Log(conflict intensity value)	0.621	0.504	0.0

Non-institutional delivery	At least one event per 100,000	0.641	0.025	-15142.2	At least one event within 50-km buffer	0.471	0.022	-46598.8
	Log(number of events per 100,000)	0.692	0.272	-186.9	Log(number of events within 50-km buffer)	0.473	0.029	-46598.8
	At least one fatality per 100,000	0.656	0.024	-6884.2	At least one fatality within 50-km buffer	0.436	0.005	-14553.1
	Log(number of fatalities per 100,000)	0.663	0.189	-4195.3	Log(number of fatalities within 50-km buffer)	0.437	0.007	-14394.5
	Log(conflict intensity value)	0.720	0.694	0.0	Log(conflict intensity value)	0.601	0.477	0.0
Missed DTP3 vaccination	At least one event per 100,000	0.482	0.023	-1219.9	At least one event within 50-km buffer	0.063	0.000	-19782.9
	Log(number of events per 100,000)	0.481	0.045	-623.6	Log(number of events within 50-km buffer)	0.069	0.000	-19779.9
	At least one fatality per 100,000	0.547	0.025	-711.2	At least one fatality within 50-km buffer	0.114	0.000	-27.0
	Log(number of fatalities per 100,000)	0.479	0.057	-158.7	Log(number of fatalities within 50-km buffer)	0.099	0.001	-30.1
	Log(conflict intensity value)	0.468	0.167	0.0	Log(conflict intensity value)	0.128	0.002	0.0

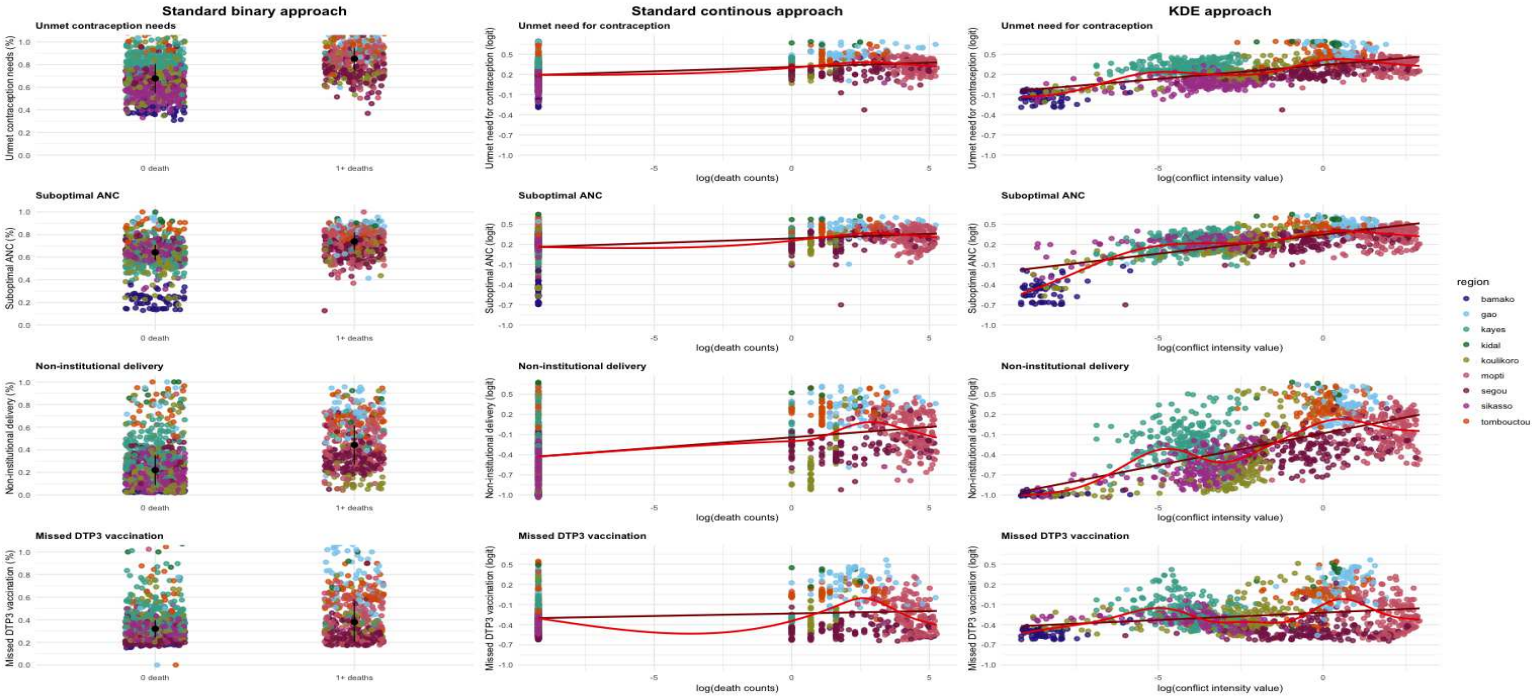
422

423

b) Health centre catchment areas

In 2013, radius-based measures in binary and continuous forms showed weak relationships with RMCH indicators (Figures S19 – 21), with Spearman correlation coefficients ranging between -0.284 and 0.053 (Table S4). The KDE-based measures revealed moderate associations, particularly with sub-optimal ANC and non-institutional delivery, with correlation coefficients of 0.65 and 0.67, respectively. The higher pseudo-R^2 and the negative AIC difference for these two RMCH indicators, along with missed DTP3 vaccine, indicate that model fit was better when conflict intensity was measured using KDE than with the standard approaches.

Moderate associations between the different conflict measures and the RMCH indicators were noted in 2018 for unmet need for contraception, suboptimal ANC, and non-institutional delivery; despite some scatter, the proportion of underuse of those services increased with conflict exposure (Figure 6). Still, the model fit metrics for the KDE-based models were better than those under the binary and continuous radius-based specifications.



438

439 **Figure 6. Association between conflict exposure measures and reproductive, maternal, and child health outcomes at the**
440 **community health center level in 2018. Legend:** The left column displays RMCH indicator (%) distributions by the binary conflict
441 exposure, defined as the occurrence of at least one fatality within a 50-km radius of a health facility. The middle column shows
442 distributions of the RMCH indicator (logit) by the number of fatalities within a 50-km radius on the log scale. The right column
443 presents distributions of the RMCH indicator (logit) by continuous conflict intensity on the log scale, estimated using kernel density
444 estimation (KDE). The linear regression lines are shown in light red, and the non-linear lines from generalized additive models are
445 shown in dark red.

DISCUSSION

Summary of findings

Armed conflicts have profound direct and indirect consequences for health and impede progress toward national and global health targets. Adopting detailed and nuanced measures of armed conflicts that capture how they propagate across space and over time is therefore critical for identifying the populations most affected and the areas where targeted efforts are needed to mitigate their adverse effects.

Using Mali as a case study, we demonstrated the use of KDE to generate high-resolution, continuous surfaces of conflict intensity by incorporating spatial and temporal bandwidths and windows, along with adjustments for conflict-related deaths and population density. These surfaces capture the spatial influence of conflict events that extend beyond the location of occurrence. We compared the number and proportion of conflict-exposed populations identified by the KDE and the common standard approaches (event and fatality rates within health district boundaries, and count of events and fatalities within a 50-km radius of health facilities). Overall, we found fair agreement in 2013 and moderate to substantial agreement in 2018 and 2023. Although conflict-exposure thresholds were set arbitrarily across approaches, the results suggest each approach measures conflict differently.

At the health district level, in 2018, KDE yielded stronger associations and better model fit for three of the four indicators, with higher correlation coefficients and R^2 values and negative AIC differences. The KDE-derived conflict exposure demonstrated a log-linear dose-response relationship between increased conflict intensity and reduced use of RMCH services. We also

noted that continuous standard metrics offered no additional nuance than the binary standard metrics. At the health facility level, the relationships between the different conflict exposures and the RMCH indicators were noisier and more scattered for both 2013 and 2018. Yet KDE-based exposure provided higher positive associations and model fit values than the standard approaches.

These results could be explained by the fact that standard methods do not account for indirect, spillover exposure beyond their predefined boundaries (health districts and fixed radius). Since boundaries are permeable and conflict actors move across them, neighboring settings are likely to share the burden of conflict exposure. As a spatial smoothing method that incorporates event proximity and influence (captured by population density and the number of fatalities), KDE provides greater spatial resolution and continuous surfaces that capture the fact that conflict exposure is not bound by artificial administrative borders or radius edges [56]. These findings align with previous research demonstrating the benefits of KDE for mapping event-based phenomena and for measuring associations with social and health outcomes [21, 57].

Public health implications

The practical implications of the KDE approach are significant. For policy and humanitarian planning, KDE-generated surfaces offer a detailed view of where conflict intensity is higher, indicating the communities most likely to experience the greatest indirect effects of conflict. This makes the KDE-based exposure estimates valuable for prioritizing resource allocation and targeting interventions. In contrast, in settings like Mali, where conflicts are widespread, using standard approaches led to classifying large areas of the territory as exposed, which is not

sufficiently nuanced to support humanitarian and public health efforts. While the primary value of KDE is to provide continuous surfaces, the values can be aggregated to administrative levels relevant for decision-making.

Most importantly, this study shows that KDE can serve as an alternative to commonly used methods for operationalizing conflict exposure and can support the examination of health effects. We found evidence of a negative ecological association between armed conflict intensity and RMCH services coverage. These findings underscore the importance of explicitly treating armed conflict as a primary exposure in quantitative studies of health outcomes in conflict-affected settings. Conducting such studies requires nuanced measures of conflict exposure, which KDE can help derive. Further research should investigate how KDE can be used to measure the association between conflict and various health outcomes through regression analyses, while adjusting for other key determinants of health. To support such analysis at fine spatial scales, the KDE values could be extracted at the level of community health worker sites, villages, or households. In addition to exploring its use in traditional epidemiological study designs, a KDE-based conflict measure could be incorporated as a primary exposure or key risk factor in geostatistical models, thus offering a critical opportunity to enhance health outcome prediction and mapping. This should be further explored, particularly in the context of infrequent censuses and large-scale household surveys [58] and increasingly constrained global health funding [59].

Strengths and limitations

A key strength of this paper is its use of georeferenced conflict event data to generate conflict-intensity surfaces that better reflect conflict dynamics than the standard approaches. We defined

several parameters to capture how conflict events propagate across space and time. We included an adaptive bandwidth to account for variation in the spatial influence with the number of events. We acknowledge the inherent subjectivity in selecting a bandwidth [46]. While the bandwidth that minimizes the MISE is typically regarded as optimal, additional work is required to address bandwidth selection across large spatio-temporal windows of multi-modal data. We also incorporated fatalities and population size to reflect that spatial spread may be greater in areas with more casualties and in less populated areas. These specifications enable us to adapt the KDE model to the Malian context. This, in turn, allowed us to better characterize how the intensity of armed conflict evolved over time and its relationship to key RMCH outcomes. Because several user-defined parameters can affect smoothness and local intensity estimates, we conducted sensitivity analyses, which showed that conflict intensity remained stable across different model specifications.

Despite these strengths, the KDE application has some limitations. Although it allows for key parameters to be specified to generate surfaces relevant to the setting of interest, these parameters are ultimately selected individually, which limits generalizability across settings. Further research is needed to determine whether KDE parameters can be standardized across conflict-affected settings to facilitate comparability. Computational time is also an important consideration. The standard approaches can be computed relatively quickly, whereas KDE may take considerably longer, depending on the number of conflict events, spatio-temporal resolution of interest, parameters specified, and available computing capacity (Table S1).

The analyses were constrained by the availability and quality of the secondary data. At the time of this study, the DHS Program had not produced modeled surfaces of the RMCH indicators for 2023. This prevented us from conducting the full comparative analysis for 2023; we only performed the comparison of population groups exposed to conflict. Moreover, georeferenced conflict event datasets are known to suffer from underreporting, especially in remote areas, and from location misclassification [38], which may have biased the conflict measures produced. Both the standard and KDE approaches can be substantially affected by underreporting and event misclassification bias. However, KDE offers some degree of robustness, as it requires a representative sample of realizations of the underlying process and smooths event locations [21], rather than relying on an exhaustive list of events, as the standard approaches do. The RMCH coverage surfaces used as outcomes also carry inherent uncertainty [40]. For example, the 2013 surfaces used DHS data from the same year, which excluded conflict-affected regions, leading to higher uncertainty in those areas. This limitation may have biased the observed associations. Still, the results share similarities with those obtained using the 2018 surfaces, which were built using nationally representative survey data.

CONCLUSIONS

Using data from Mali, this study showed that KDE can provide detailed and nuanced measures of conflict intensity for population health research. KDE-based conflict exposure indicated stronger ecological associations and improved model fit compared with the standard approaches. Future research should assess how KDE can support the examination of the health effects of armed conflicts at fine spatial scales.

LIST OF ABBREVIATIONS

AIC: Akaike Information Criterion

ANC: Antenatal care

DTP: Diphtheria, Tetanus, and Pertussis

KDE: Kernel Density Estimation

MAE: Mean Absolute Error

RMCH: Reproductive, Maternal and Child Health

RMSE: Root Mean Square Error

R^2: Coefficient of Determination

DECLARATIONS

Ethics approval and consent to participate

Ethics approval was received from both the Research Ethics Board at the University of Toronto (REB number: 43913) and Mali's National Office for Reproductive Health (ONASR).

Consent for publication

Not applicable.

Availability of data and materials

The data analysed in this study are publicly available on the ACLED (https://acleddata.com), UCDP (https://ucdp.uu.se), WorldPop (https://www.worldpop.org), and DHS (https://dhsprogram.com) websites.

Competing interests

The authors declare that they have no competing interests.

Funding

This work was conducted as part of MOO's Ph.D. thesis, which received support from the Pierre Elliott Trudeau Foundation, the Data Science Institute of the University of Toronto, and the Centre for Global Health at the University of Toronto. PMM is supported by the Fonds voor Wetenschappelijk Onderzoek – Research Foundation Flanders Senior Postdoctoral Fellowship (#1201925N). None of the funders played a role in the conceptualization, design, data collection, analysis, decision to publish, or preparation of the manuscript.

Authors' contributions

All authors contributed to the conception and design of the study. MOO analyzed the data. All authors contributed to the interpretation of the results. MOO prepared the first draft of the manuscript. All authors critically reviewed and edited manuscript drafts and approved the final version.

Acknowledgements

We thank Dr. Augustin Tapsoba for sharing his insights on implementing kernel density estimation and for sharing code snippets.

REFERENCES

1. Rustad SA. Conflict Trends: A Global Overview, 1946-2024.PRIO Paper. Oslo; 2025.
2. ACLED. Raleigh Report - December 2025. 2025.
3. UNHCR. Figures at a glance: How many refugees and forcibly displaced people are there? 2025. https://www.unhcr.org/hk/en/about-unhcr/overview/figures-glance. Accessed 10 Jan 2026.
4. Vesco P, Baliki G, Brück T, Döring S, Eriksson A, Fjelde H, et al. The impacts of armed conflict on human development: A review of the literature. World Dev. 2025;187:106806. https://doi.org/10.1016/J.WORLDDEV.2024.106806.
5. Jayasinghe S. The 12 dimensions of health impacts of war (the 12-D framework): a novel framework to conceptualise impacts of war on social and environmental determinants of health and public health. BMJ Glob Health. 2024;9:14749. https://doi.org/10.1136/BMJGH-2023-014749.
6. Checchi F. Estimation of population mortality in crisis-affected populations: Guidance for humanitarian coordination mechanisms. 2018.
7. Garry S, Checchi F. Armed conflict and public health: into the 21st century. J Public Health (Bangkok). 2020;42:e287–98. https://doi.org/10.1093/pubmed/fdz095.
8. Keasley J, Blickwedel J, Quenby S. Adverse effects of exposure to armed conflict on pregnancy: A systematic review. BMJ Global Health. 2017;2:e000377. https://doi.org/10.1136/bmjgh-2017-000377.
9. Adeyanju GC, Schrage P, Jalo RI, Abreu L, Schaub M. Armed violent conflict and healthcare-seeking behavior for maternal and child health in sub-Saharan Africa: A systematic review. PLoS One. 2025;20. https://doi.org/10.1371/JOURNAL.PONE.0317094.
10. Boerma T, Tappis H, Saad-Haddad G, Das J, Melesse DY, Dejong J, et al. Armed conflicts and national trends in reproductive, maternal, newborn and child health in sub-Saharan Africa: what can national health surveys tell us? Analysis. BMJ Glob Health. 2019;4:161–8. https://doi.org/10.1136/bmjgh-2018-001300.
11. Druetz T, Browne L, Bicaba F, Mitchell MI, Bicaba A. Effects of terrorist attacks on access to maternal healthcare services: a national longitudinal study in Burkina Faso. BMJ Glob Health. 2020;5:e002879. https://doi.org/10.1136/BMJGH-2020-002879.
12. Bendavid E, Boerma T, Akseer N, Langer A, Malembaka EB, Okiro EA, et al. The effects of armed conflict on the health of women and children. The Lancet. 2021;397:522–32. https://doi.org/10.1016/s0140-6736(21)00131-8.
13. Das JK, Padhani ZA, Jabeen S, Rizvi A, Ansari U, Fatima M, et al. Impact of conflict on maternal and child health service delivery - How and how not: A country case study of conflict affected areas of Pakistan. Confl Health. 2020;14:1–16. https://doi.org/10.1186/S13031-020-00271-3/TABLES/5.
14. David SD, Eriksson A. Association between conflict intensity and health outcomes in contemporary conflicts, while accounting for the vulnerability and functioning of healthcare services. Conflict and Health 2025 19:1. 2025;19:14-. https://doi.org/10.1186/S13031-025-00654-4.
15. Amberg F, Chansa C, Niangaly H, Sankoh O, De Allegri M. Examining the Relationship between Armed Conflict and Health Service Coverage in Sub-Saharan Africa – A Geospatial Analysis in 35 Countries. SSRN Electronic Journal. 2022;11:e843–53. https://doi.org/10.2139/ssrn.4200357.

16. Sato R. Effect of armed conflict on vaccination: Evidence from the Boko haram insurgency in northeastern Nigeria. Confl Health. 2019;13:1–10. https://doi.org/10.1186/s13031-019-0235-8.
17. Wagner Z, Heft-Neal S, Bhutta ZA, Black RE, Burke M, Bendavid E. Armed conflict and child mortality in Africa: a geospatial analysis. The Lancet. 2018;392:857–65. https://doi.org/10.1016/S0140-6736(18)31437-5.
18. Wagner Z, Heft-Neal S, Wise PH, Black RE, Burke M, Boerma T, et al. Women and children living in areas of armed conflict in Africa: a geospatial analysis of mortality and orphanhood. Lancet Glob Health. 2019;7:e1622–31. https://doi.org/10.1016/S2214-109X(19)30407-3.
19. Ngwang A, Wong KL, Banke-Thomas A. Geospatial analysis of the impact of Cameroonian Anglophone Crisis conflict intensity on antenatal care utilisation. Communications Medicine 2026 6:1. 2026;6:109-. https://doi.org/10.1038/s43856-026-01374-3.
20. Buzzelli M. Modifiable Areal Unit Problem. International Encyclopedia of Human Geography. 2019;:169. https://doi.org/10.1016/B978-0-08-102295-5.10406-8.
21. Tapsoba A. The cost of fear: Impact of violence risk on child health during conflict. J Dev Econ. 2023;160:102975. https://doi.org/10.1016/J.JDEVECO.2022.102975.
22. Chen YC. A tutorial on kernel density estimation and recent advances. Biostat Epidemiol. 2017;1:161–87. https://doi.org/10.1080/24709360.2017.1396742.
23. Jankowska MM, Natarajan L, Godbole S, Meseck K, Sears DD, Patterson RE, et al. Research article kernel density estimation as a measure of environmental exposure related to insulin resistance in breast cancer survivors. Cancer Epidemiology Biomarkers and Prevention. 2017;26:1078–84. https://doi.org/10.1158/1055-9965.EPI-16-0927.
24. Kauhl B, Schweikart J, Krafft T, Keste A, Moskwyn M. Do the risk factors for type 2 diabetes mellitus vary by location? A spatial analysis of health insurance claims in Northeastern Germany using kernel density estimation and geographically weighted regression. International Journal of Health Geographics 2016 15:1. 2016;15:38-. https://doi.org/10.1186/S12942-016-0068-2.
25. Neal S, Ruktanonchai C, Chandra-Mouli V, Matthews Z, Tatem AJ. Mapping adolescent first births within three east African countries using data from Demographic and Health Surveys: exploring geospatial methods to inform policy. Reproductive Health 2016 13:1. 2016;13:98-. https://doi.org/10.1186/S12978-016-0205-1.
26. Hu Y, Wang F, Guin C, Zhu H. A spatio-temporal kernel density estimation framework for predictive crime hotspot mapping and evaluation. Applied Geography. 2018;99:89–97. https://doi.org/10.1016/J.APGEOG.2018.08.001.
27. Govorov M, Beconytė G, Gienko G. Trivariate Kernel Density Estimation of Spatiotemporal Crime Events with Case Study for Lithuania. Sustainability 2023, Vol 15, Page 8524. 2023;15:8524. https://doi.org/10.3390/SU15118524.
28. Zombré D, Diarra D, Touré L, Bonnet E, Ridde V. Improving healthcare accessibility for pregnant women and children in the context of health system strengthening initiatives and terrorist attacks in Central Mali: a controlled interrupted time series analysis. BMJ Glob Health. 2024;7 Suppl 9:e012816. https://doi.org/10.1136/BMJGH-2023-012816.
29. Ataullahjan A, Gaffey MF, Tounkara M, Diarra S, Doumbia S, Bhutta ZA, et al. C'est vraiment compliqué: A case study on the delivery of maternal and child health and nutrition interventions in the conflict-affected regions of Mali. Confl Health. 2020;14:1–17. https://doi.org/10.1186/s13031-020-0253-6.

30. Degni F, Amara ID, Klemetti R. Women´s Experiences in Accessing Maternal and Child Health Services During the Period of the Armed Conflict in the North of Mali. Open Public Health J. 2015;8:17–22.
31. Degni F, Diallo BA, Ansari W El, Klemetti R, Valtonen K. Women's Experiences in Accessing Reproductive, Maternal, and Child Healthcare Services in the Mopti Regions of Mali. International Journal of Women's Health and Wellness . 2016;2:15.
32. Coulibaly P, Schantz C, Traoré B, Bagayoko NS, Traoré A, Chabrol F, et al. In the era of humanitarian crisis, young women continue to die in childbirth in Mali. Conflict and Health. 2021;15. https://doi.org/10.1186/s13031-020-00334-5.
33. ACLED. Armed Conflict Location & Event Data (ACLED) Codebook. 2024.
34. Raleigh C, Kishi R, Linke A. Political instability patterns are obscured by conflict dataset scope conditions, sources, and coding choices. Humanities and Social Sciences Communications 2023 10:1. 2023;10:74-. https://doi.org/10.1057/s41599-023-01559-4.
35. Davies S, Pettersson T, Sollenberg M, Öberg M. Organized violence 1989–2024, and the challenges of identifying civilian victims. Journal of Peace Research. 2025;62.
36. Sundberg R, Melander E. Introducing the UCDP Georeferenced Event Dataset. J Peace Res. 2013;50.
37. Raleigh C, Kishi R. Comparing Conflict Data: Similarities and Differences Across Conflict Datasets. 2019.
38. Eck K. In data we trust? A comparison of UCDP GED and ACLED conflict events datasets. Coop Confl. 2012;47:124–41. https://doi.org/10.1177/0010836711434463.
39. Tatem AJ. WorldPop, open data for spatial demography. Scientific Data 2017 4:1. 2017;4:170004-. https://doi.org/10.1038/sdata.2017.4.
40. Burgert-Brucker CR, Dontamsetti T, Gething PW. The DHS Program's Modeled Surfaces Spatial Datasets. Stud Fam Plann. 2018;49:87–92. https://doi.org/10.1111/SIFP.12050;JOURNAL:JOURNAL:17284465;WGROUP:STRING:PUBLICATION.
41. Gething P, Tatem A, Bird tom, Burgert-Brucker CR. Creating spatial interpolation surfaces with DHS data. Rockville, Maryland, USA: ICF International; 2015.
42. Spatial Data Repository - Modeled Surfaces. https://spatialdata.dhsprogram.com/modeled-surfaces/#survey=AL|2017|DHS. Accessed 22 Oct 2026.
43. Wigley A, Lorin J, Hogan D, Utazi CE, Hagedorn B, Dansereau E, et al. Estimates of the number and distribution of zero-dose and under-immunised children across remote-rural, urban, and conflict-affected settings in low and middle-income countries. PLOS Global Public Health. 2022;2 10 October:e0001126. https://doi.org/10.1371/journal.pgph.0001126.
44. Annuaire Statistique. Bamako; 2025.
45. Silverman BW. Density Estimation for Statistics and Data Analysis. First edition. CRC Press; 1998.
46. Moraga Paula. Spatial statistics for data science : theory and practice with R. CRC Press; 2024.
47. Davies TM, Marshall JC, Hazelton ML. Tutorial on kernel estimation of continuous spatial and spatiotemporal relative risk. Stat Med. 2018;37:1191–221. https://doi.org/10.1002/SIM.7577.
48. OCDE/CSAO. Géographie des conflits en Afrique du Nord et de l'Ouest. Paris: Éditions OCDE; 2020. https://doi.org/10.1787/4b0abf5e-fr.
49. Groupe de Recherche en Economie Appliquée et Théorique (GREAT). Résumé des résultats: Enquête d'Afrobarometer Round 10 au Mali, 2024. 2025.

50. Diggle PJ. Statistical Analysis of Spatial and Spatio-Temporal Point Patterns. 3rd edition. Chapman and Hall/CRC; 2013. https://doi.org/10.1201/b15326.
51. Ge Y, Sun M, Pu Y. Geographic information system-based edge effect correction for Ripley's K-function under irregular boundaries. Geographical Research. 2019;57:436–47. https://doi.org/10.1111/1745-5871.12363;REQUESTEDJOURNAL:JOURNAL:17455871;ISSUE:ISSUE:DOI.
52. Azzalini A, Menardi G. Clustering via Nonparametric Density Estimation: The R Package pdfCluster. J Stat Softw. 2014;57:1–26. https://doi.org/10.18637/JSS.V057.I11.
53. Baston D. exactextractr: Fast Extraction from Raster Datasets using Polygons. R package version 0.10.0. 2025.
54. McHugh ML. Interrater reliability: the kappa statistic. Biochem Med (Zagreb). 2012;22:276. https://doi.org/10.11613/bm.2012.031.
55. Beltran RS, Tarwater CE. Overcoming the pitfalls of categorizing continuous variables in ecology, evolution and behaviour. Proceedings of the Royal Society B: Biological Sciences. 2024;291:20241640. https://doi.org/10.1098/RSPB.2024.1640.
56. Carlos HA, Shi X, Sargent J, Tanski S, Berke EM. Density estimation and adaptive bandwidths: A primer for public health practitioners. Int J Health Geogr. 2010;9:1–8. https://doi.org/10.1186/1476-072X-9-39/FIGURES/9.
57. King TL, Bentley RJ, Thornton LE, Kavanagh AM. Using kernel density estimation to understand the influence of neighbourhood destinations on BMI. BMJ Open. 2016;6:e008878. https://doi.org/10.1136/BMJOPEN-2015-008878.
58. Ferreira LZ, Blumenberg C, Utazi CE, Nilsen K, Hartwig FP, Tatem AJ, et al. Geospatial estimation of reproductive, maternal, newborn and child health indicators: a systematic review of methodological aspects of studies based on household surveys. Int J Health Geogr. 2020;19:41. https://doi.org/10.1186/s12942-020-00239-9.
59. Khaki JJ, Molenaar J, Karki S, Olal E, Straneo M, Mosuse MA, et al. When health data go dark: the importance of the DHS Program and imagining its future. BMC Med. 2025;23:241. https://doi.org/10.1186/S12916-025-04062-6.

Supplementary Files

This is a list of supplementary files associated with this preprint. Click to download.

- Supplementarymaterials23Oct2026.docx